Chirality

WILEY

Chirality

RESEARCH ARTICLE

Resolution and Absolute Configuration of Fargesin Enantiomers

Eloá R. Mestriner[1] | Eric Y. Lee[2] | Camila L. Cunha[1] | Victor M. S. Sousa[2] | Isabele R. Nascimento[1] | João M. Batista Jr[2]

[1]Instituto de Química, Universidade Estadual Paulista (Unesp), Araraquara, São Paulo, Brazil | [2]Instituto de Ciência e Tecnologia, Universidade Federal de São Paulo, São José do Campos, São Paulo, Brazil

Correspondence: Isabele R. Nascimento (isabele.nascimento@unesp.br) | João M. Batista Jr (batista.junior@unifesp.br)

Received: 15 September 2024 | **Revised:** 11 October 2024 | **Accepted:** 12 October 2024

Funding: This work was supported by the Fundação de Amparo à Pesquisa do Estado de São Paulo (2023/12475-5) and the Coordenação de Aperfeiçoamento de Pessoal de Nível Superior (Finance Code 001).

Keywords: chiral chromatography | DFT | ECD | furofuran | lignans | natural products | ORD | VCD

ABSTRACT

Fargesin is an important bioactive furofuran lignan isolated from different plant species. Despite presenting potent biological activities, its stereochemical characterization has relied mostly on empirical correlations of optical rotation, an approach considered risky that commonly leads to misassignments and error propagation. Additionally, the enantiomeric purity of fargesin isolates used for biological assays has not been previously investigated. Herein, we report the enantioresolution of a scalemic mixture of fargesin isolated from *Aristolochia warmingii* along with the first unambiguous determination of the absolute configuration of each enantiomer by means of optical rotatory dispersion, as well as electronic and vibrational circular dichroism aided by quantum-chemical calculations.

1 | Introduction

Fargesin (**1**, also known as methylpluviatilol) (Figure 1) is a furofuran lignan first reported in 1972 from the dried flower buds of *Magnolia fargesii* (Magnoliaceae), one of the constituents of the Chinese traditional drug "Shin-i" [1]. Since then, numerous biological activities have been reported for fargesin, including antiprotozoal and antimycobacterial [2], anti-inflammatory [3], anticancer [4], antiathrerosclerotic [5], antiarthritic [6], antiallergic [7], allelopathic [8], among others [9]. Interestingly though, the enantiomeric purity and the absolute configuration of the tested lignans were not assessed in any of the abovementioned biological activity investigations. Although no specific rotation was provided for **1** in its first report, both dextrorotatory [10, 11] and levorotatory [12, 13] fargesin have been described from different plant species over the years, making its unambiguous stereochemical characterization critical for the correct evaluation of biological activities. Regarding the absolute configuration of fargesin, many of the assignments reported so far have been based on empirical correlations of optical rotation obtained for structurally related molecules [10, 14]. The stereo-controlled total syntheses of both racemic and (+)-fargesin have also been described [15–17]; however, the only chiroptical data provided for synthetic (+)-fargesin was its specific rotation at 589 nm.

As part of our program devoted to phytochemical investigations of Aristolochiaceae species, (−)-fargesin was recently isolated from *Aristolochia warmingii* [18]. Surprisingly, the specific rotation measured for the isolated lignan was close to zero {$[\alpha]_D^{25} = -4.0$ ($c = 0.1$, $CHCl_3$)}, in contrast with literature reports and suggesting the presence of a scalemic mixture. Scalemic mixtures are a rather common feature in natural product chemistry, although largely overlooked [19, 20]. Furofuran lignans in particular may be considered a major class of scalemic natural products with one

Eloá R. Mestriner and Eric Y. Lee contributed equally as first authors.

interesting example being pinoresinol, for which different enantiomers can accumulate in different organs of the same plant [20]. That prompted us to evaluate the enantiomeric purity of **1** by means of chiral HPLC, which led to the semipreparative resolution of fargesin enantiomers. With both enantiomers in hands, it was possible to unambiguously assign their absolute configurations using optical rotatory dispersion (ORD), electronic (ECD), and vibrational circular dichroism (VCD) spectroscopies associated with density functional theory (DFT) calculations. This is the first report of the isolation of a scalemic mixture of fargesin, its enantioresolution, and the unambiguous assignment of the absolute configuration of its enantiomers by means of chiroptical spectroscopy and quantum-chemical calculations. This approach has practical advantages when compared to stereoselective total synthesis, besides providing information about both the absolute configuration and preferential conformations in solution-state.

2 | Materials and Methods

2.1 | Plant Material and Fargesin Isolation

The procedures for the isolation of fargesin from *Aristolochia warmingii* (Aristolochiaceae) as well as its structural identification and relative configuration assignment using NMR and MS data were described in Reference [18].

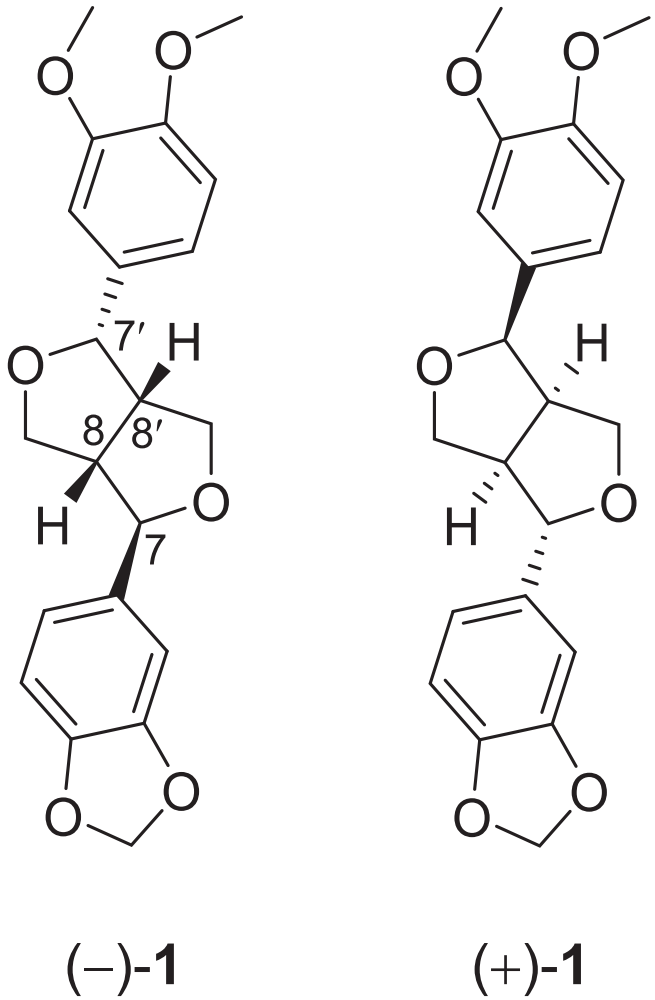

FIGURE 1 | Chemical structures of fargesin (**1**) enantiomers.

2.2 | General

The chiral HPLC analyses were performed using a JASCO chromatograph equipped with a LC-NetII/ADC controller, PU-2086 Plus pumps, AS-2055 Plus automatic injector, CO-2060 Plus column thermostat, and MD-2018 Plus photodiode array and CD-2095 Plus detectors. Enantioresolutions were performed on a CHIRALCEL® OD-RH column (Daicel, 4.6×150 mm, 5 μm), ACN/H_2O 50:50, 1 mL min^{-1} flow rate, λ = 280 nm ([−]-**1** at 15.25 min and [+]-**1** at 18.74 min), CHIRALPAK® IC column (Daicel, 4.6×250 mm, 5 μm), Hex/EtOH 80:20, 1 mL min^{-1} flow rate, λ = 280 nm ([−]-**1** at 34.66 min and [+]-**1** at 56.67 min) and Lux Cellulose-1 column (Phenomenex®, 4.6×250 mm, 5 μm), Hex/EtOH 75:25, 1 mL min^{-1} flow rate, λ = 280 nm ([−]-**1** at 16.85 min and [+]-**1** at 25.79 min). Fargesin (**1**, 15.0 mg) was submitted to semipreparative separation using CHIRALCEL® OD-RH column to give (−)-**1** (6.6 mg) and (+)-**1** (6.0 mg).

ORD was measured in chloroform, acetonitrile, and methanol, at 589, 578, 546, 436, 405, and 365 nm, using a Jasco P2000 polarimeter equipped with sodium and mercury lamps, along with appropriate filters. Sample concentration was kept at 0.25 mg mL^{-1}, and the optical rotation was recorded using a cylindrical glass sample cell of 1 dm pathlength and 10 mm ID. OR values were reported as a mean of three to five measurement blocks of five repetitions each. IR and VCD experimental spectra were recorded simultaneously with a BioTools dual-PEM Chiral*IR*-2X FT-VCD spectrometer using a resolution of 4 cm^{-1} and a collection time of 12 h. The optimum retardation of the ZnSe photoelastic modulators (PEMs) was set at 1400 cm^{-1}. The IR and VCD spectra of fargesin enantiomers were recorded in $CDCl_3$ solution (4.0 mg in 130 mL) in a BaF_2 cell with 100 μm path length. Minor instrumental baseline offsets were eliminated by subtracting the VCD spectra of the enantiomers followed by division by 2 (half difference). The UV and ECD spectra of fargesin enantiomers were recorded with a Jasco J-850 spectrometer in the 210- to 400-nm region using the following parameters: bandwidth 0.5 nm; response 1 s; scanning speed 100 nm min^{-1}; three accumulations; room temperature (25°C); sample in methanol and acetonitrile solutions; 0.1 cm cell path length; and concentration 0.1 mg mL^{-1}.

2.3 | Chiroptical Properties Calculations

The conformational search of fargesin (**1**) was carried out at the molecular mechanics level of theory employing both the MM+ and MMFF force fields incorporated in HyperChem 8.0.10 and Spartan 08 software packages, respectively. The DFT calculations were carried out at 298 K in either chloroform or acetonitrile solutions using the polarizable continuum model (PCM) in its integral equation formalism version (IEFPCM), incorporated in Gaussian 09 software [21]. The configuration 7*R*,8*S*,7′*S*,8′*S* was arbitrarily chosen for **1** based on the relative configuration described in ref 18. The VCD, ECD, and OR properties of its enantiomer were obtained by multiplying the calculated data by (−1). Initially, 36 conformers were identified for **1** within a 10 kcal mol^{-1} energy window. These conformers were then geometry optimized at the B3PW91/PCM ($CHCl_3$)/6-311G(d,p) and B3PW91/PCM(ACN)/6-311G(d,p) levels. The five ($CHCl_3$) and four (ACN) lowest energy conformers of **1**,

with relative energy (rel E.) < 2.0 kcal/mol, were selected for IR/VCD, UV/ECD and OR calculations. IR and VCD were simulated at the B3PW91/PCM($CHCl_3$)/6-311G(d,p) level, and the spectra were created using dipole and rotational strengths from Gaussian, which were converted into molar absorptivity ($M^{-1}\,cm^{-1}$). Each spectrum was plotted as a sum of Lorentzian bands with half-widths at half-maximum (HWHM) of 6 cm^{-1}. The calculated wavenumbers were multiplied with a scaling factor of 0.975, and the Boltzmann-average-composite IR and VCD spectra were plotted using Origin software. UV and ECD spectra for **1** were calculated at the CAM-B3LYP/PCM(ACN)/TZVP on geometries obtained at the B3PW91/PCM (ACN)/6-311G(d,p) level. Vibrational analysis at the level used for geometry optimizations resulted in no imaginary frequencies for all conformers, confirming them as real minima. TDDFT was employed to calculate the excitation energy (in nm) and rotatory strength *R* in the dipole velocity (R_{vel} in cgs units: 10^{-40} $esu^2\,cm^2$) form. The calculated rotatory strengths from the first 30 singlet → singlet electronic transitions were simulated into an ECD curve using Gaussian bands with HWHM of σ 0.15 eV. The predicted wavelength transitions were multiplied with a scaling factor of 1.06, determined by the best agreement between the experimental and calculated UV spectra, and the composite spectra were plotted as Boltzmann averages of the lowest-energy conformers (CAM-B3LYP/PCM(ACN)/TZVP electronic energies). ORD properties were calculated at 589, 578, 546, 436, 405, and 365 nm at the B3LYP/6−311++(d,p) level in chloroform and acetonitrile solutions using PCM. Discrete specific rotation values at each wavelength of individual conformers were Boltzmann averaged using B3PW91/6-311G(d,p) Gibbs free energies.

3 | Results and Discussion

The furofuran lignan fargesin was isolated from the leaves of *Aristolochia warmingii* (Aristolochiaceae) [18]. As the specific rotation measured for the isolated lignan was close to zero {$[\alpha]_D^{25} = -4.0$ ($c = 0.1$, $CHCl_3$)}, we proceeded with the development of a chiral HLPC method for the investigation of its enantiomeric purity. Enantioresolution of **1** was observed using a CHIRALCEL® OD-RH (Daicel) column. Peak areas indicated a small excess (~4%) of the levorotatory lignan. Similar separation conditions have already been described for other furofuran lignans [22–27]. Semipreparative purification of the enantiomers of fargesin was then performed, and the separated enantiomers were analyzed using CHIRALPAK® IC (Daicel) and Lux Cellulose-1 (Phenomenex®) columns. Chromatograms are presented in the Supporting Information (Figures S1–S5).

As previously mentioned, the absolute configuration of fargesin was originally assigned by means of empirical comparisons of specific rotation recorded for structurally related compounds [10, 14]. These assignments were based on the important work of Freudenberg and Sidhu [28] who, in the early 1960s, investigated the absolute configuration of sesamin and pinoresinol derivatives through chemical correlation and optical rotation studies. They concluded that dextrorotatory furofuran lignans had *R*-configured bridge carbons C-8 and C-8′, whereas the etherified carbons C-7 and C-7′ could be deduced by means of the shift rule of the optical rotation. Following this empirical rule, the authors of References [10] and [14] assigned the absolute configuration of (+)-fargesin as 7*S*,8*R*,7′*R*,8′*R*. It is important to mention, however, that in Reference [10], the relative configuration of fargesin (methylpluviatilol, compound 8) was drawn incorrectly. Given the lack of an unambiguous assignment of the absolute configuration of fargesin enantiomers by means of chiroptical spectroscopy, herein, we use a combination of chiroptical methods associated with quantum-chemical calculations for the stereochemical investigation of **1**. Because most of the assignments were based on optical rotation, the first chiroptical property investigated was ORD. In order to assess the impact of different solvents on the specific rotation of **1**, measurements were performed in chloroform, methanol, and acetonitrile. The results obtained at 589 nm in chloroform for the (+)-enantiomer were similar to that reported in the literature {$[\alpha]_D^{24} = +103.3$ ($c = 0.014$, $CHCl_3$), lit. $[\alpha]_D^{20} = +112.7$ ($c = 1.1$, $CHCl_3$) [29]}; however, the specific rotation observed for the isolated (−)-enantiomer was significantly larger than literature results, indicating a scalemic mixture for the latter {$[\alpha]_D^{23} = -127.5$ ($c = 0.017$, $CHCl_3$), lit. $[\alpha]_D^{25} = -54.7$ ($c = 0.3$, $CHCl_3$) [12]}. Experimental ORD results were compared to calculated data at six discrete wavelengths, 589, 578, 546, 436, 405, and 365 nm. The experimental dispersion curves observed for (−)-**1** in chloroform and acetonitrile presented similar profiles and specific rotation magnitudes (Figure 2 and Table S1), suggesting similar conformations for **1** in these solvents. The dispersion curve obtained in methanol, however, presented some discrepancies in the lower wavelength region (Figure S6). The very good correlation between experimental and calculated ORD data both in chloroform and acetonitrile (Figure 2) allowed the assignment of (−)-**1** as 7*R*,8*S*,7′*S*,8′*S*, in accordance with literature results.

The second chiroptical method used to investigate the stereochemistry of **1** was ECD. UV and ECD spectra of fargesin enantiomers were recorded both in methanol and acetonitrile, resulting in almost superimposable spectra (Figures 3 and S7). TDDFT calculations were performed at the CAM-B3LYP/PCM(ACN)/TZVP, and the very good correlation between experimental and calculated data (Figure 3) led to the assignment

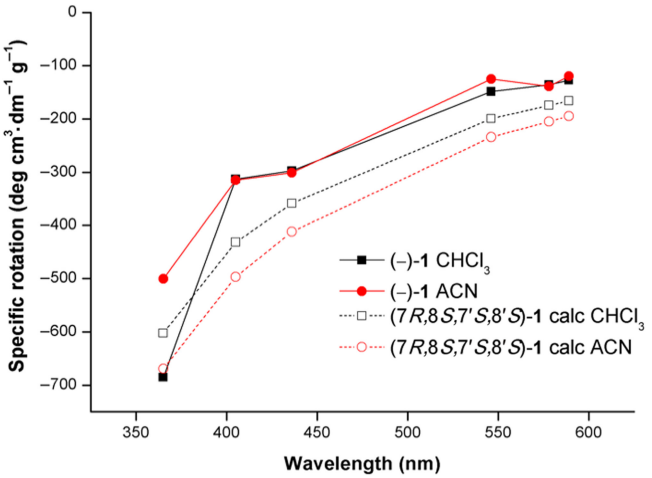

FIGURE 2 | Comparison of experimental ORD of (−)-fargesin (**1**) in chloroform and acetonitrile with calculated [B3LYP/PCM($CHCl_3$ or ACN)/6−311++(d,p)] data for 7*R*,8*S*,7′*S*,8′*S*-**1**. See ESI for lowest energy conformers.

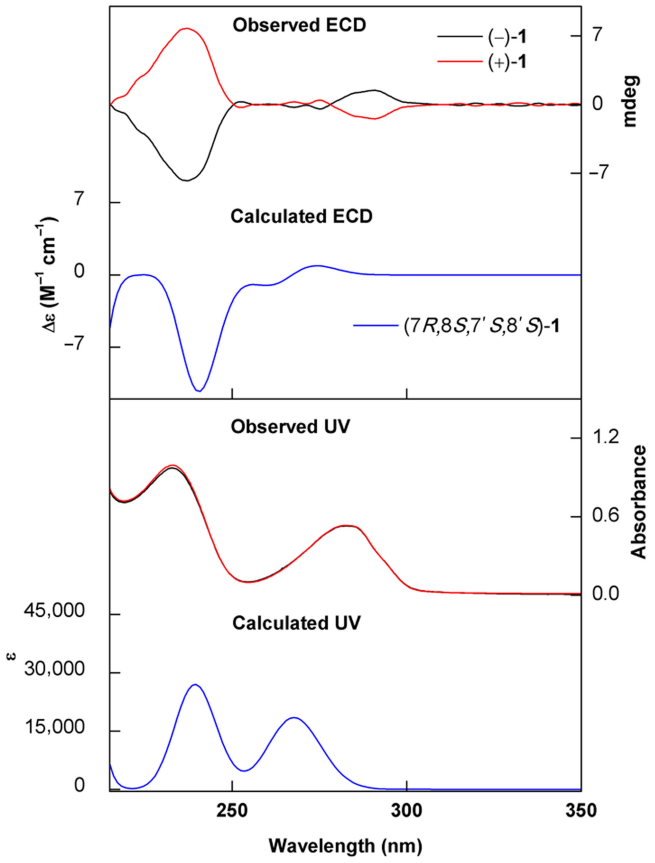

FIGURE 3 | Comparison of experimental UV and ECD spectra of fargesin (**1**) enantiomers in acetonitrile with calculated [CAM-B3LYP/PCM(ACN)/TZVP] data for 7*R*,8*S*,7′*S*,8′*S*-**1**. See ESI for lowest energy conformers.

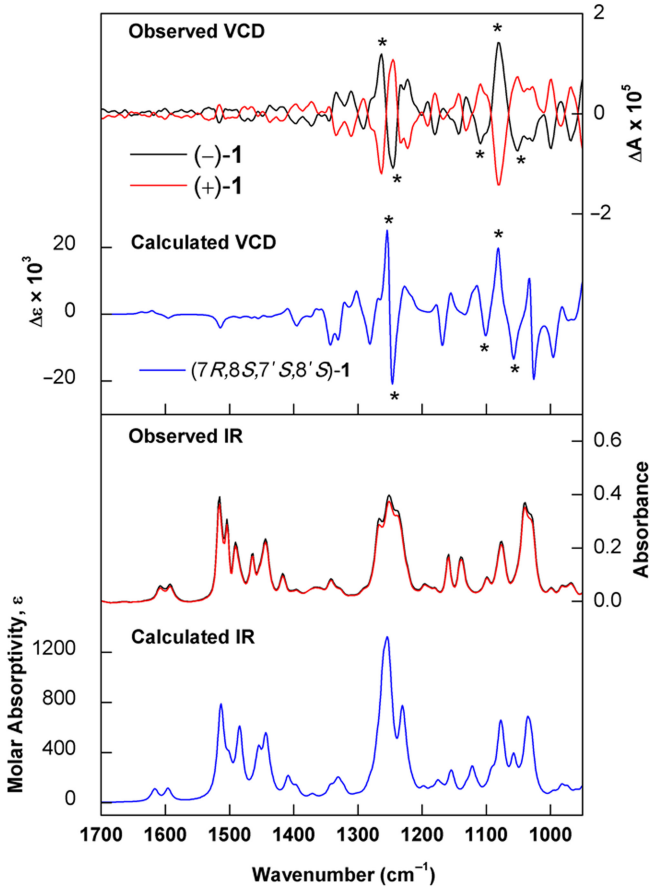

FIGURE 4 | Comparison of experimental IR and VCD spectra of fargesin (**1**) enantiomers in $CDCl_3$ with calculated [B3PW91/PCM($CHCl_3$)/6–311G(d,p)] data for 7*R*,8*S*,7′*S*,8′*S*-**1**. See ESI for lowest energy conformers. Asterisks represent selected band assignments.

of (–)-fargesin as 7*R*,8*S*,7′*S*,8′*S* and, consequently, (+)-fargesin as 7*S*,8*R*,7′*R*,8′*R*, corroborating ORD results. The Cotton effects (CE) at around 240 and 290 nm present in the ECD spectra of the enantiomers of **1** are also commonly observed for structurally related lignans. Their exact excitation energy and relative signs, however, seem to vary depending both on the relative configuration of the bicyclic tetrahydrofurofuran moiety as well as the aromatic rings substitution patterns [24–26, 28]. Analysis of natural transition orbitals (NTO) involved in the electronic transitions of the above-mentioned ECD bands revealed the Cotton effects at 290 nm (CE+) and 240 nm (CE–) in 7*R*,8*S*,7′*S*,8′*S*-**1** to arise from n-π* and π-π* transitions involving both substituted aromatic rings (MO98 HOMO to MO99 LUMO and MO97 HOMO-1 to MO100 LUMO+1) (Figure S8). Investigation of the canonical orbitals underlying the negative CE at 240 nm also indicated charge transfer components between the two aromatic rings (MO97 HOMO-1 to MO100 LUMO+1, MO97 HOMO-1 to MO102 LUMO+3, and MO98 HOMO to MO101 LUMO+2) (Figure S9).

Finally, VCD spectroscopy was employed to assess the absolute configuration of fargesin enantiomers. Excellent agreements were observed between experimental and calculated spectra (Figure 4) leading to the assignment of (–)-**1** as 7*R*,8*S*,7′*S*,8′*S* and (+)-**1** as 7*S*,8*R*,7′*R*,8′*R*, corroborating ORD and ECD results. The main features observed in the experimental spectra, namely, the –, +, – band pattern centered at 1080 cm^{-1} and the couplet like signal –, + centered at 1250 cm^{-1} were found to arise mostly from C-C and C-O stretches along with CH_2 rocking of the bicyclic furofuran ring for the lower wavenumber feature, whereas the 1250 cm^{-1} couplet involved C-O stretches of the aromatic ring substituents coupled with in-plane aromatic C-H bendings as well as methine C-H bendings of the stereogenic carbons of the furofuran moiety. The more localized vibrations directly comprising the stereocenters of the molecule make VCD a more sensitive and reliable tool for stereochemical investigations of this class of compounds. Although VCD has been applied to a large variety of secondary metabolites [30], no previous reports on the use of VCD for absolute configuration assignments of furofuran lignans were found in the literature.

4 | Conclusion

A scalemic mixture of the furofuran lignan fargesin was reported for the first time from *Aristolochia warmingii*. Its enantiomeric resolution as well as the assignment of the absolute configuration of each enantiomer was achieved by means of chiral HPLC, chiroptical spectroscopy, and quantum-chemical calculations.

Even though the absolute configuration reported in the literature based on empirical correlations, and further supported by stereoselective total synthesis, was proven correct, the results presented herein demonstrate the importance of assessing the enantiomeric purity of furofuran lignans as well as using a combination of chiroptical methods and DFT calculations for their stereochemical investigations. The unambiguous assignment of the absolute configuration of fargesin enantiomers as (−)-(7*R*,8*S*,7′*S*,8′*S*)-**1** and (+)-(7*S*,8*R*,7′*R*,8′*R*)-**1** is very relevant considering the plethora of biological activities reported for this compound and the general lack of correlation between stereochemistry and biological potential. Further structural and stereochemical investigations of furofuran lignans will benefit from the wealth of information provided by electronic and vibrational chiroptical spectroscopies aided by quantum-chemical calculations.

Author Contributions

Eloá R. Mestriner: investigation, methodology, formal analysis. **Eric Y. Lee:** investigation, methodology, formal analysis. **Camila L. Cunha:** supervision, validation. **Victor M. S. Sousa:** investigation, methodology. **Isabele R. Nascimento:** supervision, resources, validation, writing – original draft, writing – review and editing. **João M. Batista Jr:** conceptualization, supervision, funding acquisition, writing – original draft, writing – review and editing.

Acknowledgments

This work was supported by grants from Fundação de Amparo à Pesquisa do Estado de São Paulo – FAPESP (Grant 2023/12475-5) and by resources supplied by the Centre for Scientific Computing (NCC/GridUnesp) of São Paulo State University (Unesp). C.L.C thanks Coordenação de Aperfeiçoamento de Pessoal de Nível Superior – CAPES (Finance Code 001).

References

1. H. Kakisawa, Y. P. Chen, and H. Y. Hsü, "Lignans in Flower Buds of *Magnolia fargesii*," *Phytochemistry* 11 (1972): 2289–2293.

2. A. Jiménez-Arellanes, R. León-Díaz, M. Meckes, et al., "Antiprotozoal and Antimycobacterial Activities of Pure Compounds From *Aristolochia elegans* Rhizomes," *Evidence-Based Complementary and Alternative Medicine* 2012 (2012): 593403.

3. T.-H. Pham, M.-S. Kim, M.-Q. Le, et al., "Fargesin Exerts Anti-Inflammatory Effects in THP-1 Monocytes by Suppressing PKC-Dependent AP-1 and NF-κB Signaling," *Phytomedicine* 24 (2017): 96–103.

4. G.-E. Lee, C.-J. Lee, H.-J. An, et al., "Fargesin Inhibits EGF-Induced Cell Transformation and Colon Cancer Cell Growth by Suppression of CDK2/Cyclin E Signaling Pathway," *International Journal of Molecular Sciences* 22 (2021): 2073.

5. G. Wang, J.-H. Gao, L.-H. He, et al., "Fargesin Alleviates Atherosclerosis by Promoting Reverse Cholesterol Transport and Reducing Inflammatory Response," *Biochimica et Biophysica Acta - Molecular and Cell Biology of Lipids* 1865 (2020): 158633.

6. J. Lu, H. Zhang, J. Pan, et al., "Fargesin Ameliorates Osteoarthritis via Macrophage Reprogramming by Downregulating MAPK and NF-κB Pathways," *Arthritis Research & Therapy* 23 (2021): 142.

7. P. T. L. Hong, H. J. Kim, W. K. Kim, and J. H. Nam, "*Flos magnoliae* Constituent Fargesin Has an Anti-Allergic Effect via ORAI1 Channel Inhibition," *Korean Journal of Physiology & Pharmacology* 25 (2021): 251–258.

8. A. L. Anaya, M. Macías-Rubalcava, R. Cruz-Ortega, et al., "Allelochemicals From *Stauranthus perforatus*, a Rutaceous Tree of the Yucatan Peninsula, Mexico," *Phytochemistry* 66 (2005): 487–494.

9. K. Patel and D. K. Patel, "Biological Potential and Therapeutic Effectiveness of Phytoproduct 'Fargesin' in Medicine: Focus on the Potential of an Active Phytochemical of *Magnolia fargesii*," *Recent Advances in Inflammation & Allergy Drug Discovery* 18 (2024): 79–89, https://doi.org/10.2174/0127722708286664240429093913.

10. M. W. Biavatti, P. C. Vieira, M. F. G. F. Silva, et al., "Separation and NMR Studies on Lignans of *Raulinoa echinata*," *Phytochemical Analysis* 12 (2001): 64–68.

11. D.-X. Li, M. Liu, and X.-J. Zhou, "A New Dimeric Lignan From *Zanthoxylum simulans*," *Zhongguo Zhong Yoa Za Zhi* 40 (2015): 2843–2848.

12. G. B. Messiano, L. Vieira, M. B. Machado, L. M. X. Lopes, S. A. Bortoli, and J. Zucherman-Schpector, "Evaluation of Insectcidal Activitiy of Diterpenes and Lignans From *Aristolochia malmeana* Against *Anticarsia gemmatalis*," *Journal of Agricultural and Food Chemistry* 56 (2008): 2655–2659.

13. T. Guo, D. Su, Y. Huang, Y. Wang, and Y.-H. Li, "Ultrasound-Assisted Aqueous Two-Phase System for Extraction and Enrichment of *Zanthoxylum armatum* Lignans," *Molecules* 20 (2015): 15273–15286.

14. H. Greger and O. Hofer, "New Unsymetrically Substituted Tetrahydrofurofuran Lignans From *Artemisia absinthium*: Assignment of the Relative Stereochemistry by Lanthanide Induced Chemical Shifts," *Tetrahedron* 36 (1980): 3551–3558.

15. R. C. D. Brown, C. J. R. Bataille, G. Bruton, J. D. Hinks, and N. A. Swain, "C–H Insertion Approach to the Synthesis Ofendo,exo-Furofuranones: Synthesis of (±)-Asarinin, (±)-Epimagnolin A, and (±)-Fargesin," *The Journal of Organic Chemistry* 66 (2001): 6719–6728.

16. T. Ogiku, S.-i. Yoshida, M. Takahashi, T. Kuroda, H. Ohmizu, and T. Iwasaki, "A New Stereocontrolled Synthesis of Axial-Equatorial Furofuran Lignans Having Two Different Aryl Groups: A Synthesis of Fargesin," *Tetrahedron Letters* 33 (1992): 4477–4478.

17. S.-i. Yoshida, T. Yamanaka, T. Miyake, Y. Moritani, H. Ohmizu, and T. Iwasaki, "Asymmetric Syntheses of Lignans Utilizing Novel Diastereoselective Michael Addition of Cyanohydrin: Syntheses of (+)-Fargesin and (−)-Picropodophyllone," *Tetrahedron* 53 (1997): 9585–9598.

18. C. L. Cunha, P. V. G. Antonio, M. C. G. Lustosa, et al., "Warminins A, B and C, Three new Furofuran Lignans From *Aristolochia warmingii* Mast. (Aristolochiaceae)," *Journal of the Brazilian Chemical Society* 34 (2022): 1071–1077.

19. A. N. L. Batista, F. M. Santos, Jr., J. M. Batista, Jr., and Q. B. Cass, "Enantiomeric Mixtures in Natural Product Chemistry: Separation and Absolute Configuration Assignment," *Molecules* 23 (2018): 492.

20. S. Mazzotta, V. Rositano, L. Senaldi, A. Bernardi, P. Allegrini, and G. Appendino, "Scalemic Natural Products," *Natural Product Reports* 40 (2023): 1647–1671.

21. M. J. Frisch, G. W. Trucks, H. B. Schlegel, et al., *Gaussian 09 (Revision A.02)* (Wallingford CT: Gaussian, Inc., 2009).

22. K.-W. Kim, S. G. A. Moinuddin, K. M. Atwell, M. A. Costa, L. B. Davin, and N. G. Lewis, "Opposite Stereoselectivities of Dirigent Proteins in *Arabidopsis* and *Schizandra* Species," *The Journal of Biological Chemistry* 287 (2012): 33957–33972.

23. Y. Lu, Y. Xue, J. Liu, et al., "(±)-Acortatarinowins A–F, Norlignan, Neolignan, and Lignan Enantiomers From *Acorus tatarinowii*," *Journal of Natural Products* 78 (2015): 2205–2214.

24. W.-J. Liu, Y.-J. Chen, D.-N. Chen, et al., "A New Pair of Enantiomeric Lignans From the Fruits of *Morinda citrifolia* and Their Absolute Configuration," *Natural Product Research* 32 (2018): 933–938.

25. L. Zhou, F.-Y. Han, L.-W. Lu, et al., "Isolation of Enantiomeric Furolactones and Furofurans From *Rubus idaeus* L. With Neuroprotective Activities," *Phytochemistry* 164 (2019): 122–129.

26. J. K. Hwang, S. G. A. Moinuddin, L. B. Davin, and N. G. Lewis, "Pinoresinol-Lariciresinol Reductase: Substrate Versatility, Enantiospecificity, and Kinetic Properties," *Chirality* 32 (2020): 1–20.

27. J. Wang, L. Zhou, Z.-Y. Cheng, et al., "Chiral Resolution and Bioactivity of Enantiomeric Furofuran Lignans From *Juglans mandshurica* Maxim," *Natural Product Research* 34 (2020): 2225–2228.

28. K. Freudenberg and G. S. Sidhu, "Die Absolute Konfiguration der Gruppe des Sesamins und Pinoresinols," *Chemische Berichte* 94 (1961): 851–862.

29. Y. Seo, "Antioxidant Activity of the Chemical Constituents From the Flower Buds of *Magnolia denudata*," *Biotechnology and Bioprocess Engineering* 15 (2010): 400–406.

30. A. N. L. Batista, A. L. Valverde, L. A. Nafie, and J. M. Batista, Jr., "Stereochemistry of Natural Products From Vibrational Circular Dichroism," *Chemical Communications* 60 (2024): 10439–10450.

Supporting Information

Additional supporting information can be found online in the Supporting Information section.